



Tropical rainforest biodiversity and aboveground carbon changes and uncertainties in the Selva Central, Peru



Patrick Gonzalez ^{a,*}, Benjamín Kroll ^b, Carlos R. Vargas ^c

^a Center for Forestry, University of California, Berkeley, CA 94720-3114, USA

^b ECOYUNGAS, Rioja, San Martín, Peru

^c Facultad de Ciencias Forestales, Universidad Nacional Agraria La Molina, Lima, Peru

ARTICLE INFO

Article history:

Received 30 July 2013

Received in revised form 10 October 2013

Accepted 14 October 2013

Available online 6 November 2013

Keywords:

Climate change

Deforestation

Forest carbon

Landsat

Monte Carlo analysis

REDD+

ABSTRACT

Tropical deforestation has reduced the extent of natural forests, which conserve biodiversity, provide essential resources to people, and reduce climate change by storing carbon. Forest conservation projects need tree species data to effectively manage biodiversity while greenhouse gas reduction programs require robust methods to estimate forest carbon. Here, we use field measurements, remote sensing, and Monte Carlo analyses to quantify tree biodiversity and aboveground carbon changes and uncertainties in 5200 km² of Amazonian and Yungas rainforest and other land around the Parque Nacional Yanachaga-Chemillén and two other protected areas in the Selva Central, Peru. Field inventories of 17 ha found 438 tree species in 156 families. Field measurements of 10,838 trees and Monte Carlo analyses of uncertainties in measurements, allometric equations, wood density, and the carbon fraction of biomass showed that aboveground live carbon densities were 93 ± 39 Mg ha⁻¹ (mean \pm 95% confidence interval [CI]) in old-growth forest and 40 ± 10 Mg ha⁻¹ in secondary forest. Carbon density was significantly correlated to tree species richness ($P < 0.0001$). Supervised classification of Landsat images showed a 1989–2005 net deforestation rate of $0.3\% \text{ y}^{-1}$, reduction of forest cover from three-quarters of the area to two-thirds, and net degradation of additional forest equivalent to half the deforested area. A Monte Carlo analysis that combined carbon density and remote sensing uncertainties showed that forest changes caused statistically significant net emissions of 1.6 ± 0.4 million Mg carbon. Allometric equations and remote sensing accounted for most of the uncertainty. Multivariate statistical analyses showed that, of six factors examined, distance to roads most explained historical deforestation patterns. The protected areas experienced no net deforestation, very low degradation, and very low change close to roads. Projection of potential forest cover to 2021 indicates that a Reducing Emissions from Deforestation and Degradation (REDD+) project could avoid gross emissions of 2.8 ± 0.8 million Mg carbon. One-eighth of the area would be eligible for afforestation or reforestation under the Clean Development Mechanism (CDM), with credit for carbon storage occurring above a projected baseline gross reforestation rate of $1.8\% \text{ y}^{-1}$. These activities could conserve tropical forest carbon and biodiversity.

© 2013 Elsevier B.V. All rights reserved.

1. Introduction

Tropical forests protect globally unique biodiversity, provide wood, water, food, and other vital resources to local people, and help reduce climate change by storing carbon. Tropical countries contain a majority of the world's endemic plant species (Joppa et al., 2011), old-growth tropical forests are the most species-rich in the world (Gibson et al., 2011), and this biodiversity enhances the forest productivity that sustains many people (Cardinale et al., 2012).

* Corresponding author.

E-mail address: pgonzalez@cal.berkeley.edu (P. Gonzalez).

Tropical forests also remove substantial quantities of greenhouse gases from the atmosphere, reducing the magnitude of climate change. Tropical forests removed carbon from the atmosphere at a 1990–2007 rate of 2.8 ± 0.4 Gt y⁻¹ (mean \pm SD; Pan et al., 2011), compared to 2002–2011 global fossil fuel emissions of 8.3 ± 0.4 Gt y⁻¹ and global deforestation emissions of 1.0 ± 0.5 Gt y⁻¹ (Le Quéré et al., 2013).

Tropical deforestation is the main source of land for agricultural expansion (Gibbs et al., 2010), although industrial timber harvesting accounts for half of the wood removed in South America (FAO, 2011). Deforestation fragments tropical ecosystems, causing declines of old-growth tree species (Laurance et al., 2006) and isolating national parks and other areas that protect biodiversity (DeFries et al., 2005). The ability of resource managers to track

the effects of forest management actions on biodiversity depends on monitoring the distribution and abundance of species.

To encourage forest conservation, the United Nations Framework Convention on Climate Change (UNFCCC) is developing a REDD+ program to create credits for avoided deforestation that buyers could use to offset fossil fuel emissions. The UNFCCC CDM currently certifies credits from afforestation and reforestation activities. The credibility of these and other greenhouse gas reduction programs rests on the development of scientifically robust methods to quantify the forest carbon stored due to project activities.

A forest inventory that counts and measures individual trees is the most direct method to quantify forest carbon. Financial costs, however, render forest inventory infeasible as the sole method for large areas. Remote sensing, calibrated by field measurements, provides data to produce spatial estimates of carbon across extensive areas. Only a few remote sensing efforts, however, have produced wall-to-wall spatial estimates of forest carbon across the tropics. These include estimates of aboveground live carbon stocks at 500 m spatial resolution using Moderate Resolution Imaging Spectroradiometer (MODIS) and Geoscience Laser Altimeter System (GLAS) data (Baccini et al., 2012) and at 1 km spatial resolution using GLAS data (Saatchi et al., 2011) and an estimate of 2000–2005 carbon emissions at 18.5 km spatial resolution using MODIS data (Harris et al., 2012). The spatial resolutions of these efforts are too coarse to effectively inform forest and carbon management decisions for landscape-scale projects of a few thousand square kilometers. Instead, analyses of Landsat data at 30 m spatial resolution can produce spatial estimates of forest carbon useful for small areas (Asner et al., 2010).

The potential errors and variation of remote sensing data, allometric biomass equations, and other key components of forest carbon estimation render necessary a careful quantification of uncertainty. This is necessary to ascertain if estimated net changes in greenhouse gas emissions and removals over time are statistically significant. A net change might be considered significant if the entire range (central estimate \pm 95% CI) of estimated values of a net greenhouse gas change are less than zero (emissions) or greater than zero (removals). In addition, quantification of the contribution of individual variables to uncertainty can point to how strengthening specific links in the chain of methods could reduce overall uncertainty. To quantify uncertainty, the Intergovernmental Panel on Climate Change (IPCC, 2006) recommends Monte Carlo analysis, yet only a few forest carbon research efforts have applied this approach (e.g. Gonzalez et al., 2010a; Monni et al., 2007).

We seek to demonstrate a method to address the concurrent need for tree species information and forest carbon data and the need to quantify uncertainty for REDD+ and CDM carbon estimates. Our research examines an area of high tree biodiversity and biomass in Peru that lacks spatial data on forest carbon. The research objectives are: (1) to quantify tree biodiversity based on field inventories in the Selva Central, Peru, (2) to quantify historical land cover and forest carbon changes and uncertainties, based on field measurements of individual trees, Landsat remote sensing, and Monte Carlo analyses, and (3) to project potential future forest carbon changes and uncertainties.

2. Methods

2.1. Research area

The research area is 5200 km² of tropical rainforest and other land between 9.85° and 10.82° S and 74.98° and 75.79° W in the Selva Central, Peru, a region at the western end of the Amazon Basin that extends up the east slope of the Andes Mountains (Fig. 1).

The research area forms a buffer zone of private land to the west of three areas protected by the government: the Parque Nacional Yanachaga-Chemillén (national park, established 1986), Reserva Comunal Yanesha (communal reserve, established 1988), and Bosque de Protección San Matías-San Carlos (protection forest, established 1987).

A warm, humid climate extends over most of the research area, with a rainy season from November to April. Mean annual temperature and total annual precipitation (1901–2002) range from, respectively, 23 °C and 2300 mm y⁻¹ (lowlands) to 14 °C and 770 mm y⁻¹ (mountain slopes) (Gonzalez et al., 2010b; Mitchell and Jones, 2005).

Elevation (Appendix) differentiates the flora of Selva Central into four principal vegetation types: Selva Baja (lowland Amazonian rainforest), Yungas (low elevation montane rainforest), Ceja de la Montaña (mid-elevation cloud forest), and Puna (high elevation alpine grassland) (Brako and Zarucchi, 1993; Gentry, 1993; Richards, 1996). The unique topography and ecology of the Selva Central has fostered a high level of plant endemism, with up to 30% of plant species native only to Peru (Brako and Zarucchi, 1993) and endemics occurring at a density of 13 species per 1000 km² (van der Werff and Consiglio, 2004). Many epiphytic and terrestrial orchids bloom in the Yungas and become most prevalent and diverse in the Ceja de la Montaña (Gentry, 1993). The restricted elevation range of many tree species renders the Selva Central highly vulnerable to upslope vegetation shifts due to climate change (Gonzalez et al., 2010b).

In the national park, the Servicio Nacional de Áreas Naturales Protegidas por el Estado (SERNANP) does not allow resource extraction. The park provides habitat to over 400 bird and 80 mammal species, including *Tremarctos ornatus* (the spectacled bear). In the protection forest, SERNANP allows some direct use of non-wood forest products, but always under specific management plans. In the communal reserve, the Yanesha control natural resource management and have effectively excluded resource extraction, although economic pressures are changing traditional practices (Hamlin and Salick, 2003). The human population density is relatively low, although a long history of human occupation has altered much of the Selva Central (Santos-Granero and Barclay, 1998; Appendix).

The location of the research area originated with the interest of the Government of Peru and the local non-governmental organization Fundación Peruana para la Conservación de la Naturaleza (ProNaturaleza) in reducing deforestation in the private lands surrounding the national park. Therefore, we defined the project area as the Selva Baja, Yungas, and Ceja de la Montaña areas that surround the national park and communal reserve on the west side of the protection forest. We set the other borders of the project at ecological boundaries: Puna grassland to the west, the Río Pozuzo and the Río Huampumayo in the north, the Río Paucartambo in the south, and mountain ridges to the northwest and the southwest.

2.2. Field measurements

To determine tree species richness and average carbon densities of old-growth and secondary forest, we established 18 field inventory plots covering 16.6 ha (Table A1). We stratified the plots into the two forest classes that Landsat satellite sensors would be able to distinguish – old-growth forest and secondary forest. Old-growth forest is closed-canopy, primary forest with multiple tiers of vegetation, never harvested or harvested more than 100 years ago (Richards, 1996). Secondary forest is open-canopy forest with one or two tiers of vegetation, regenerating naturally after abandonment of agriculture or pasture. The Selva Central secondary forest plots have been regenerating 10–42 years. The sample was not

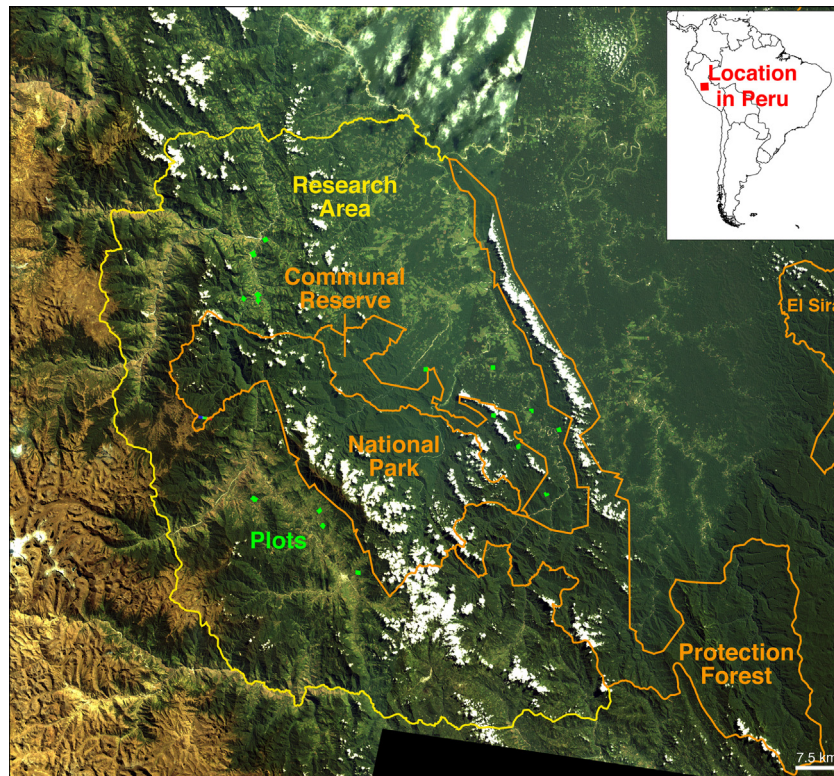


Fig. 1. Selva Central research area in a real-color Landsat image. Plots = field inventory plot locations. National Park = Parque Nacional Yanachaga-Chemillén, Communal Reserve = Reserva Comunal Yanesha, Protection Forest = Bosque de Protección San Matías-San Carlos, El Sira = Reserva Comunal El Sira (not analyzed here).

random. We chose parcels dispersed throughout the research area that represented the general physiognomy and structure of old-growth and secondary forest in the zone. A local resident with whom ProNaturaleza had worked owned each parcel. We established plots that were square or as rectangular as possible, dividing each plot into 20 m × 20 m square sub-plots.

In 2005, field crew members identified the species or lowest known taxonomic level of every live tree with a diameter at breast height (d_{bh} ; at height $[h] = 1.3$ m) ≥ 10 cm, measured d_{bh} , and nailed an aluminum tag at $h = 1.4$ m. (For ease of reference, Table A2 lists all variables.)

We compiled a list of the tree species, checking local names against Aróstegui (1974) and scientific names with records of the Missouri Botanical Garden (Brako and Zarucchi, 1993; Tropicos database <<http://www.tropicos.org>>). We also classified species as late- or early-successional, using published surveys (Laurance et al., 2004; Nelson et al., 1999; Peña-Claros, 2003; Richards, 1996; Terborgh et al., 1996; Uhl et al., 1988) and field observations.

We weighted tree data by plot area when calculating research area averages. To compare across plots, we standardized species and family richness to 1 ha with the species-area relationship, using A (area) = 1 ha and z (species-area slope) = 0.205 (Sólymos and Lele, 2012). We also recorded the α -, β -, and γ -diversity (Whittaker, 1972).

2.3. Forest carbon densities from tree measurements and Monte Carlo analysis

From field measurements, we calculated the carbon mass per unit area (carbon density) of aboveground biomass of each plot and the averages for the old-growth and secondary forest plots. We used five allometric equations developed for Amazon forest or specific Amazonian tree species (Table 1) to calculate the

biomass of each tree (b_{tree}). Because variation in wood density determines spatial patterns in Amazonian forest biomass (Baker et al., 2004a), the allometric equations include a term to scale the results by the wood density of the species of the measured tree (Aróstegui, 1974; Chave et al., 2004, 2006; Fearnside, 1997). For unidentified species, we calculated the mean wood density of all trees of known taxonomy, separately for late- and early-successional species, and applied those wood densities to trees of unknown species in old-growth and secondary forest plots, respectively.

Aboveground tree biomass density of a plot (B_{plot} , Mg ha⁻¹) equals:

$$B_{plot} = \sum_{trees} \left(\frac{b_{tree}}{A_{plot}} \right) \left(\frac{1 \text{ Mg}}{10^3 \text{ kg}} \right) \quad (1)$$

where b_{tree} (kg tree⁻¹) is from Table 1 and A_{plot} is the area (ha) of the plot.

Aboveground tree carbon density of a forest type ($C_{forest \text{ type}}$, Mg ha⁻¹) is the area-weighted average of the carbon densities of individual plots:

$$C_{forest \text{ type}} = f_C \sum_{plots} \left(\frac{A_{plot}}{A_{forest \text{ type}}} \right) B_{plot} \quad (2)$$

where $A_{forest \text{ type}}$ is the total area (ha) of all plots in either old-growth or secondary forest and f_C is the carbon fraction of biomass (0.47 g carbon [g biomass]⁻¹; McGroddy et al., 2004).

To quantify the uncertainty of each estimate of $C_{forest \text{ type}}$, we conducted a Monte Carlo analysis that evaluated error from four potential sources: variation or error of tree diameter measurement, statistical uncertainty of tree allometric equations, variation of wood density, and variation of the carbon fraction of biomass.

Table 1
Allometric equations to calculate biomass from measurements of individual trees.

Forest type or species	b_{tree}	ρ_{eq}	r^2_{adj}	P	SE_a	SE_b	SE_{old}	Source
a. Old-growth <i>terra firme</i> Amazon forest	$(\rho_{sp}/\rho_{eq}) \text{Exp}(-0.37 + 0.333 \ln d_{bh} + 0.933 (\ln d_{bh})^2 - 0.122 (\ln d_{bh})^3)$	0.67	0.97	–	–	–	0.297	Baker et al. (2004b) and Chambers et al. (2001)
b. Secondary <i>terra firme</i> Amazon forest	$(\rho_{sp}/\rho_{eq}) \text{Exp}(-1.9968 + 2.4128 \ln d_{bh})$	0.54	0.98	<0.0001	0.061	0.0273	–	Nelson et al. (1999)
c. <i>Bellucia</i> spp. (family Melastomataceae)	$(\rho_{sp}/\rho_{eq}) \text{Exp}(-1.8158 + 2.37 \ln d_{bh})$	0.54	0.99	<0.0001	0.0944	0.0403	–	Nelson et al. (1999)
d. <i>Cecropia sciadophylla</i> (family Cecropiaceae)	$(\rho_{sp}/\rho_{eq}) \text{Exp}(-2.5118 + 2.4257 \ln d_{bh})$	0.39	0.98	<0.0001	0.1986	0.069	–	Nelson et al. (1999)
e. <i>Laetia procera</i> (family Flacourtiaceae)	$(\rho_{sp}/\rho_{eq}) \text{Exp}(-2.2244 + 2.5105 \ln d_{bh})$	0.64	0.99	<0.0001	0.112	0.0483	–	Nelson et al. (1999)

b_{tree} = aboveground biomass of a tree (kg tree⁻¹), d_{bh} = diameter at breast height (at height = 1.3 m) (cm), $\text{Exp}(x) = e^x$, P = probability, ρ_{eq} = wood density of the original allometric equation (g cm⁻³), ρ_{sp} = wood density of the species of the measured tree (g cm⁻³), r^2_{adj} = adjusted coefficient of determination, $SE_{a,b}$ = Standard error of the coefficients a or b (where $b_{tree} = (\rho_{sp}/\rho_{eq}) \text{Exp}(-a + b \ln d_{bh})$), SE_{old} = Standard error of old-growth biomass (fraction of mean value).

We generated 100 realizations of b_{tree} for each tree, adding error terms to the original values of variables:

$$\hat{b}_{tree} = f(\rho_{sp} + X_{\rho}SE_{\rho}, d_{bh} + X_{dbh}SE_{dbh}, a + X_aSE_a, b + X_bSE_b) \quad (3)$$

where the hat symbol “^” denotes the form of a variable that includes a modeled estimate of error, $X_{variable}$ is a random number (different for each variable) from a normal distribution with mean = 0 and standard deviation (SD) = 1, $SE_{variable}$ = standard error of a variable, $f(variables)$ denotes allometric equations in Table 1, and ρ_{sp} , a, b = variables in Table 1b–e. SE_{ρ} comes from Aróstegui (1974) and Chave et al. (2004). Wood density standard errors not found in those sources was estimated as 10% of the mean. SE_a and SE_b come from Table 1b–e. We estimated SE_{dbh} (cm) as half of the difference of the two diameter measurements. In effect, the repeated realizations of b_{tree} simulated the potential results of 100 field campaigns.

Because the form of the allometric equation for old-growth forest species (Table 1a) is different, its Monte Carlo equation is:

$$\hat{b}_{tree} = b_{tree} + X_{mean}SE_{old} \quad (4)$$

where b_{tree} and SE_{old} are listed in Table 1a.

For each plot, we calculated 100 realizations of B_{plot} and 100 realizations of $C_{forest\ type}$:

$$C_{forest\ type} = (f_c + X_{f_c}SE_{f_c}) \sum \left(\frac{A_{plot}}{A_{forest\ type}} \right) B_{plot} \quad (5)$$

where SE_{f_c} is estimated from McGroddy et al. (2004) as 0.01 g carbon [g biomass]⁻¹.

The 95% confidence interval (CI) equals:

$$95\% \text{ CI} = \frac{C_{forest\ type}^{97.5} - C_{forest\ type}^{2.5}}{2} \quad (6)$$

where $C_{forest\ type}^{97.5}$ and $C_{forest\ type}^{2.5}$ are the 97.5th and 2.5th percentiles, respectively, of the 100 realizations of $C_{forest\ type}$. The uncertainty is the 95% CI expressed as a fraction of the mean:

$$\text{Uncertainty}_{stock} = \frac{95\% \text{ CI}}{C_{forest\ type}} \quad (7)$$

We analyzed the sensitivity of uncertainty of aboveground forest carbon density to the values of each variable by repeating the calculation four times, each time setting the error terms of all but one of the four variables (wood density [SE_{ρ}]), diameter measurement [SE_{dbh}], allometric equations [SE_a, SE_b, SE_{old}], carbon fraction [SE_{f_c}] to zero.

2.4. Historical land cover change

We used Landsat satellite Global Land Survey data (Gutman et al., 2013) to determine the spatial locations and extent of vegetation types. We calibrated the spectral bands, conducted atmospheric, radiometric, and topographic correction, and produced seamless mosaics of the research area for 1989 and 2005 (Appendix). Because much of the research area is tropical cloud forest, the Landsat scenes had unavoidable areas of cloud cover, preventing analysis of areas under clouds. To produce spatial data of 1989 and 2005 land cover, we conducted supervised classification of the Landsat mosaics. To reduce classification error, we kept the classification to a limited number of land cover classes: (1) sparse vegetation (Puna grasslands and newly cleared fields), (2) low vegetation (taller grasslands and agricultural fields), (3) secondary forest, and (4) old-growth forest. Using a real-color Landsat mosaic and field observations, we defined training areas for each vegetation class, evenly distributed across the mosaic. We conducted maximum likelihood supervised classification on the seven corrected Landsat spectral bands, performing several iterations to correct for errors.

We conducted change detection (Nelson and Holben, 1986) by comparing the two mosaics and classifying differences into four land cover change classes: (1) forest remaining forest, (2) reforestation, (3) deforestation, and (4) non-forest remaining non-forest. We also identified areas of forest degradation as areas of old-growth forest converted to secondary forest.

To assess classification accuracy, we compared our 1989–2005 deforestation and degradation areas with 2000–2004 deforestation and disturbance areas from a Landsat analysis by Oliveira et al. (2007) that overlapped 17% of our research area on the eastern side. The data from Oliveira et al. (2007) provided a much larger sample (797,262 pixels) than the field inventory (18 plots). We also compared our four 2005 land cover classes at 30 m spatial resolution to similar 2005 Globcover land cover classes at 300 m spatial resolution (Bicheron et al., 2008).

We examined the probabilities and relative weights of different factors in explaining historical patterns of forest cover change in the Selva Central: (1) distance to non-forest (for deforestation), (2) distance to forest (for reforestation), (3) elevation, (4) slope, (5) distance to rivers, (6) distance to roads, and (7) distance to villages or towns. We produced curves of the probabilities of deforestation and reforestation as a function of each factor (Appendix). We also determined the parameters of curves of standard error to produce three versions of each probability curve: the central estimate, the estimate using SE_{lower} (hereafter low), and the estimate using SE_{upper} (hereafter high). We conducted Principal Components Analyses to quantify the weight of each factor in explaining historical deforestation and reforestation (Appendix).

To assess the impact of the three protected areas on deforestation and forest degradation patterns, we analyzed rates of change in the parts of the Selva Central research area and each protected area within 5 km of roads.

2.5. Historical carbon changes from Landsat, field measurements, and Monte Carlo analysis

We combined the Landsat and field inventory results in a Monte Carlo framework to calculate the amount of aboveground live carbon in the research area and changes over time. The previously quantified measurement and carbon density calculation errors (Section 2.3) propagated through the calculation of carbon amounts, which included an additional source of uncertainty, namely, remote sensing-derived land cover classification error. In this way, we evaluated the major sources of uncertainty identified in the IPCC National Greenhouse Gas Inventory Guidelines (Aalde et al., 2006).

The total carbon stock of the research area ($c_{\text{research area}}$, Mg) equals:

$$C_{\text{research area}}^{\text{year}} = \sum_{\text{land cover classes}} A_{\text{class}}^{\text{year}} C_{\text{class}} \quad (8)$$

$C_{\text{old-growth forest}}$ and $C_{\text{secondary forest}}$ come from Eq. (2). For low vegetation, we used published results for shifting cultivation and crop-fallows in Peru: $C_{\text{low vegetation}} = 12 \text{ Mg ha}^{-1}$ (Palm et al., 2004). For sparse vegetation, we used published results for Puna grassland in Peru: $C_{\text{sparse vegetation}} = 7.1 \text{ Mg ha}^{-1}$ (Gibbon et al., 2010). These are standardized to $f_c = 0.47$.

To quantify uncertainty, we calculated 100 realizations of aboveground live carbon stock in the research area for 1989 and 2005:

$$\hat{C}_{\text{research area}}^{\text{year}} = \sum_{\text{land cover classes}} (A_{\text{class}}^{\text{year}} + X_{\text{area}} SE_{\text{area}}) (C_{\text{class}} + X_{\text{class}} SE_{\text{class}}) \quad (9)$$

where A_{class} comes from the Landsat-derived land cover classification (Section 2.4) and SE_{area} (ha) comes from the fractional error of our deforestation classification against the deforestation classification of Oliveira et al. (2007) ($e_{\text{classification}}$):

$$SE_{\text{area}} = A_{\text{class}}^{\text{year}} e_{\text{classification}} \quad (10)$$

For each realization of $c_{\text{research area}}$, we calculated A_{class} in the sequence old-growth forest-secondary forest-low vegetation-sparse vegetation, so that the total calculated area would equal the area of the research area:

$$A_{\text{sparse}}^{\text{year}} = A_{\text{research area}} - \sum_{\text{old, secondary, low}} A_{\text{class}}^{\text{year}} \quad (11)$$

For $SE_{\text{old-growth forest}}$ and $SE_{\text{secondary forest}}$, we used the previous Monte Carlo results (Section 2.3). We also used $SE_{\text{low vegetation}} = 2 \text{ Mg ha}^{-1}$ (Palm et al., 2004) and $SE_{\text{sparse vegetation}} = 0.7 \text{ Mg ha}^{-1}$ (Gibbon et al., 2010), standardized to $f_c = 0.47$. Eqs. (6) and (7) give the forms to calculate the 95% CI and fractional uncertainty of $c_{\text{research area}}$.

The 1989–2005 net carbon change of the research area ($\Delta c_{\text{research area}}$, Mg) equals:

$$\Delta c_{\text{research area}}^{1989-2005} = \sum_{\text{land cover classes}} (A_{\text{class}}^{2005} - A_{\text{class}}^{1989}) C_{\text{class}} \quad (12)$$

We calculated 100 realizations of the 1989–2005 gross carbon change of the research area:

$$\Delta \hat{c}_{\text{research area}}^{1989-2005} = \sum_{\text{land cover classes}} (|A_{\text{class}}^{2005} - A_{\text{class}}^{1989}| + X_{\text{area}} SE_{\text{area}}) (C_{\text{class}} + X_{\text{class}} SE_{\text{class}}) \quad (13)$$

Eq. (6) gives the 95% CI of the gross carbon change. Uncertainty of the gross carbon change equals:

$$\text{Uncertainty}_{\text{change}} = \frac{95\% \text{ CI}_{\text{gross}}}{\sum_{\text{land cover classes}} |A_{\text{class}}^{2005} - A_{\text{class}}^{1989}| C_{\text{class}}} \quad (14)$$

For Eqs. (13) and (14), we use the absolute value of the change in land cover area to avoid a calculation that would inaccurately cause uncertainty to reach high values as the changes in land cover area approached zero.

The 95% CI of the 1989–2005 net carbon change of the research area equals:

$$95\% \text{ CI}_{\text{net}} = \text{Uncertainty}_{\text{change}} \Delta c_{\text{research area}}^{1989-2005} \quad (15)$$

We analyzed the sensitivity of uncertainty of net carbon change to the values of each variable by repeating the calculation five times, each time setting the error terms of all but one of the five variables (wood density [SE_{ρ}]), diameter measurement [SE_{dbh}], allometric equations [SE_a , SE_b , SE_{old}], carbon fraction [SE_{f_c}], remote sensing accuracy [SE_{area}]) to zero.

2.6. Projection of potential future land cover and carbon

To estimate potential future carbon benefits of a REDD+ forest conservation project and a CDM afforestation or reforestation activity, we projected potential future land cover. We based the projections solely on the historical patterns shown by the land cover change detection and projected into the future only a period of time equal to the historical period (16 years). We conducted two analyses (deforestation and reforestation) in parallel. With the curves of the probabilities of deforestation and reforestation as a function of seven factors and the Principal Components Analysis-derived weights for each factor in explaining historical deforestation and reforestation (Appendix), we calculated central, high, and low probabilities of deforestation and reforestation for each pixel in 2021 (Appendix).

From these probabilities, we produced central, high, and low estimated spatial data layers of projected 2021 land cover and 2005–2021 land cover change (Appendix). Because the probability curves for the seven factors derived only from data in the research area, we produced projected data only for the research area. To calculate projected carbon stocks, changes, and uncertainties, we used the previous Monte Carlo methods (Section 2.5), with one modified term:

$$SE_{\text{area}} = A_{\text{class}}^{2021} e_{\text{classification}} + SE_{\text{projection}} \quad (16)$$

where $SE_{\text{projection}}$ (ha) is the higher of the differences between high and central and low and central estimates.

3. Results

3.1. Tree biodiversity

The field inventory of 10,838 trees of $d_{\text{bh}} \geq 10 \text{ cm}$ found 438 tree species, 115 genera, and 65 families (Table A3). Of the species, 71 were identifiable only to the family level, 22 identifiable only by local name, and other unidentified species were combined into

Table 2

Selva Central forest characteristics from field measurements of live trees with a diameter at breast height (d_{bh} , at $h = 1.3$ m) ≥ 10 cm. Tree density (mean), tree diameter and biomass (mean \pm SD), and aboveground carbon density (mean \pm 95% CI) are calculated by weighting each tree by its plot area. Aboveground carbon density uncertainty is calculated using Monte Carlo analysis.

Forest type	Plots (ha)	Area (ha)	Trees	Species richness			Family richness			Tree density			d_{bh} (cm)	Basal area (m ² ha ⁻¹)	Biomass (Mg tree ⁻¹)	Carbon density (Mg ha ⁻¹)
				Total (species)	Early	Late	Total (families)	Early	Late	Total (trees ha ⁻¹)	Early	Late				
Old-growth	5	4.0	3049	313	80	233	58	28	51	762	148	615	28 \pm 46	41	0.32 \pm 0.78	93 \pm 39
Secondary	13	12.6	7789	241	124	117	50	37	30	618	461	157	19 \pm 22	17	0.14 \pm 0.19	40 \pm 10
All	18	16.6	10,838	438	156	282	65	38	52	653	386	267	22 \pm 35	23	0.19 \pm 0.45	53 \pm 16

early = early-successional, late = late-successional.

separate classes for old-growth and secondary forest. Over two-thirds of the species occur at a density <1 tree ha⁻¹. Average plot species richness is 108 species ha⁻¹ (range 80–141 species ha⁻¹) in the old-growth forest plots and 43 species ha⁻¹ (range 30–76 species ha⁻¹) in the secondary forest plots. Old-growth forest hosts more late-successional species and families and more total species and families than secondary forest (Table 2). Conversely, secondary forest contains more early-successional species and families. The α -diversity (species richness of an individual plot) ranges from 29 to 141 species. The β -diversity (fraction of total species shared between old-growth and secondary forest) is 0.26. The γ -diversity (species richness of the entire landscape) is 438 species.

The family with the most trees (area-weighted) and the highest total biomass in the old-growth forest plots is *Fabaceae* (legume family). In the secondary forest plots, *Melastomataceae* (Melastome family) has the most trees and *Fabaceae* has the highest total biomass. The dominant species in the old-growth forest plots, by number, is *Iriartea deltoidea* (*camona*, family *Arecaceae*) and, by total biomass, *Pouteria torta* (*caimito*, family *Sapotaceae*). In the secondary forest plots, *Jacaranda copaia* (*charapach*, family *Bignoniaceae*) is the dominant species by number and total biomass. The inventory only recorded one *Swietenia macrophylla* (big-leaf mahogany, *caoba*, family *Meliaceae*), listed as vulnerable on the Red List of the International Union for the Conservation of Nature.

In the old-growth forest sites, 70% of aboveground biomass resides in late-successional species and 30% in early-successional species. Conversely, 30% of the biomass in the secondary forest sites rests in early-successional species and 70% in late-successional species. Aboveground live carbon shows significant correlation ($r_{adj}^2 = 0.74$, $P < 0.0001$, $n = 18$) with species richness (Fig. 2).

3.2. Forest carbon densities and uncertainties

In the old-growth forest plots, tree density is one-quarter higher than in the secondary forest plots (Table 2). Average tree diameter is also greater in the old-growth forest plots, but variation is also greater. The largest tree measured was a *Ceiba pentandra* (*lupuna*, family *Malvaceae*) with a diameter of 1.6 m and estimated carbon mass of 3.3 Mg, in old-growth forest.

Aboveground live carbon density in trees of $d_{bh} \geq 10$ cm in old-growth forest is double the carbon density in secondary forest, although the uncertainty of the estimate is also double (Table 3). The minimum carbon density estimated in the old-growth forest plots was higher than the maximum carbon density estimated in the secondary forest plots.

Standard errors, averaged over all trees, were 5.3% for diameter measurement and 10% for wood density. Wood density (mean \pm SE) ranged from 0.14 ± 0.01 g cm⁻³ (*Ochroma pyramidale*; Fearnside, 1997) to 1.04 ± 0.04 g cm⁻³ (*Manilkara bidentata*; Aró-

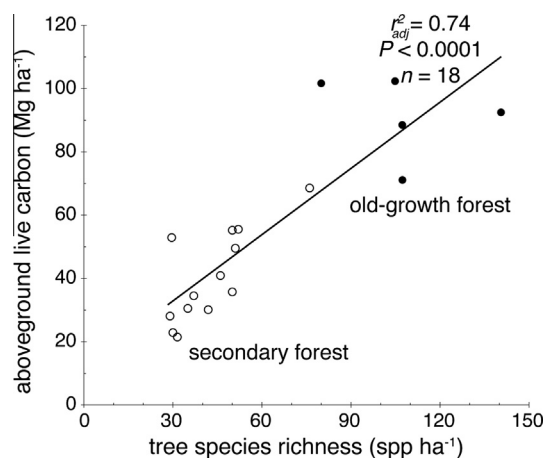


Fig. 2. Significant correlation of aboveground live carbon density in trees of $d_{bh} \geq 10$ cm with tree species richness.

Table 3

Aboveground forest carbon densities (Mg ha⁻¹) from field measurements, with uncertainty calculated by Monte Carlo analyses.

	Carbon (Mg ha ⁻¹)	95% CI (Mg ha ⁻¹)	95% CI (%)
<i>Old-growth forest</i>			
Maximum	102	43	42
Minimum	71	27	38
Mean	93	39	42
<i>Secondary forest</i>			
Maximum	69	19	27
Minimum	21	6	26
Mean	40	10	24

stegui, 1974). The standard error for the old-growth allometric equation is 30% (Chambers et al., 2001). For a secondary forest tree of $d_{bh} = 19$ cm (field inventory average) and $\rho_{sp} = 0.54$ g cm⁻³ (equation average; Nelson et al., 1999), the standard error of biomass would be 14%. From the sensitivity analysis, the allometric equations accounted for over four-fifths of the uncertainty of the forest carbon density estimates (Table A4).

3.3. Historical land cover and carbon changes

Old-growth forest covered three-quarters of the research area in 1989, decreasing to two-thirds in 2005 (Table 4). Although extensive areas of high-carbon density old-growth forest remain (Fig. 3), deforestation is widespread (Fig. 4).

Comparison of our 1989–2005 deforestation area with the 2000–2004 deforestation area of Oliveira et al. (2007) showed 85% agreement. Comparison of our forest degradation area with

Table 4
Land cover and land change in the national park (Parque Nacional Yanachaga-Chemillén), communal reserve (Reserva Comunal Yanasha), protection forest (Bosque de Protección San Matías-San Carlos), and the Selva Central research area that forms a buffer zone around the three protected areas.

Area	1989			2005			1989–2005						Rates of change						
	Total (km ²)	Cloud-free (km ²)	Old-growth (%)	Second. (%)	Low vegetation (%)	Sparse vegetation (%)	Old-growth (%)	Second. (%)	Low vegetation (%)	Sparse vegetation (%)	Forest (%)	Reforestation (%)	Deforestation (%)	Non-forestation (%)	Net reforestation (% y ⁻¹)	Net deforestation (% y ⁻¹)	Net degradation (% y ⁻¹)	Gross deforestation (% y ⁻¹)	Gross reforestation (% y ⁻¹)
National park	1100	600	96	2	1	1	96	3	1	0.5	97	2	1	0.5	-0.05	0.04	0.06	0.06	4.5
Communal reserve	320	210	98	1	0.4	0.7	97	2	0.9	0.2	98	0.9	0.9	0.2	-0.002	0.06	0.05	0.05	5.0
Protection forest	1490	530	98	0.9	0.6	0.7	96	3	0.8	0.4	98	1	1	0.2	-0.01	0.1	0.06	0.06	5.5
Research area	5180	4110	73	10	12	6	67	11	16	6	73	5	9	13	0.3	0.2	0.6	0.6	1.6

old-growth = old-growth forest, second. = secondary forest

the forest disturbance area of Oliveira et al. (2007) showed 90% agreement. Comparison of our four land cover classes for 2005 at 30 m spatial resolution with similar Globcover (Bicheron et al., 2008) classes for 2005 at 300 m spatial resolution showed 65% agreement.

The analyses of deforestation and reforestation vs. seven possible causal factors produced bivariate curves of probability vs. variable value (Figs. A1 and A2). The Principal Components Analyses identified three explanatory principal components and gave the following weights for, respectively, deforestation and reforestation: distance to non-forest (deforestation 0.173), distance to forest (reforestation 0.174), elevation (0.137, 0.180), slope (0.139, 0.147), distance to rivers (0.153, 0.142), distance to roads (0.212, 0.181), distance to villages or towns (0.186, 0.176).

Old-growth forest covers over 95% of the three protected areas, which experienced no net deforestation from 1989 to 2005. The national park and communal reserve experienced almost no net forest degradation. Degradation in the protection forest occurred at half the rate of degradation in the research area. Within 5 km of the road, deforestation rates in the research area, national park, communal reserve, and protection forest were, respectively, 0.7, 0.06, 0.03, and 0.1% y⁻¹ and forest degradation rates were, respectively, 0.5, 0.2, 0.1, and 0.2% y⁻¹.

Across the cloud-free part of the research area, the average 1989–2005 net carbon change was -3.9 ± 1.0 Mg ha⁻¹ and the total change was -1.6 ± 0.4 million Mg (Table 5). Areas of complete loss of old-growth forest lost up to 93 ± 39 Mg ha⁻¹ of carbon. Uncertainties of carbon stock estimates were one-quarter of the mean values, while uncertainty of the carbon change estimate was slightly more than one-third of the mean (Table 5). Remote sensing inaccuracy accounted for almost all of the uncertainty of the carbon change estimate (Table A4).

3.4. Projected future land cover and carbon changes and uncertainties

Calculations project old-growth forest covering 63% of the research area in 2021 and 2005–2021 net deforestation of 0.2% y⁻¹, net degradation of an additional 0.2% y⁻¹, gross deforestation of 0.7% y⁻¹, and gross reforestation of 1.8% y⁻¹ (Fig. 5). Projected carbon changes (Table 5) are similar in magnitude, but higher in uncertainty, than calculated historical changes.

4. Discussion

4.1. Biodiversity

The Selva Central old-growth forest sites have more tree species per unit area than many tropical forests, including one-third of 25 tropical forest sites (range 56–283 species ha⁻¹) examined in a pan-tropical analysis (Phillips et al., 1994), and more tree species than 26 temperate forest sites (range 13–226 species, 1700–740,000 ha) examined in a pan-temperate analysis (Latham and Ricklefs, 1993). The Selva Central old-growth forest sites have one-third fewer species and families, however, than lowland old-growth Amazonian forest sites farther to the east in an area documented as the most tree species-rich in the world (Gentry, 1988; Laurance et al., 2004; Pitman et al., 2002; Terborgh and Andresen, 1998). Those Amazonian plots are protected in national parks, so it is notable that old-growth forest on private land in the Selva Central still conserves high species richness. The Selva Central β -diversity is in the middle of the range for neotropical rainforests (Condit et al., 2002). The dominance of *I. deltoidea* over other species and *Fabaceae* over other families in Selva Central old-growth forest is consistent with other Amazonian forests (Pitman et al., 2002; Terborgh and Andresen, 1998).

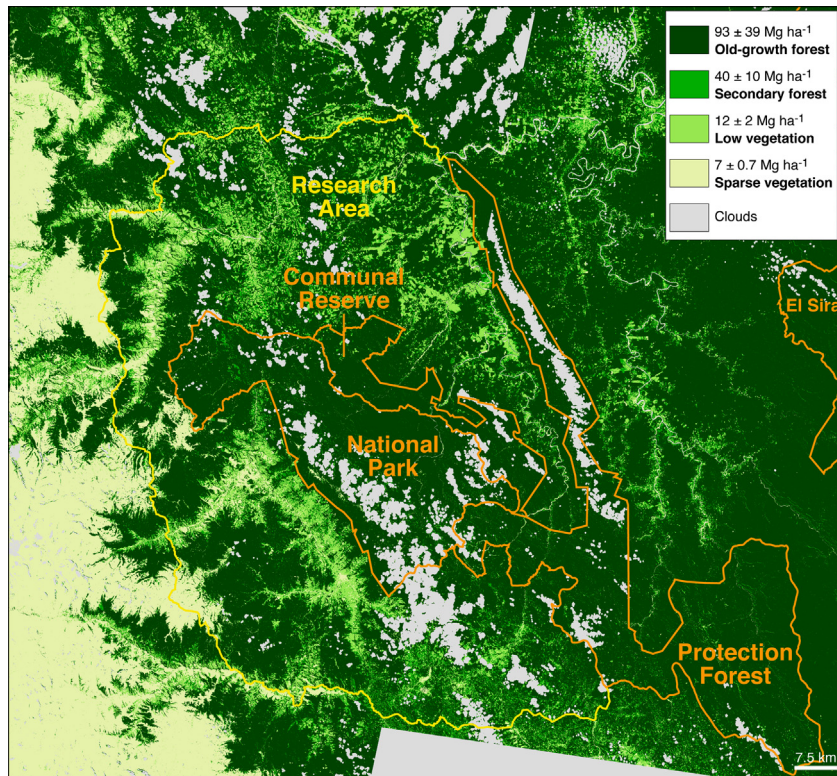


Fig. 3. Aboveground live carbon in trees of $d_{bh} \geq 10$ cm and land cover in 2005.

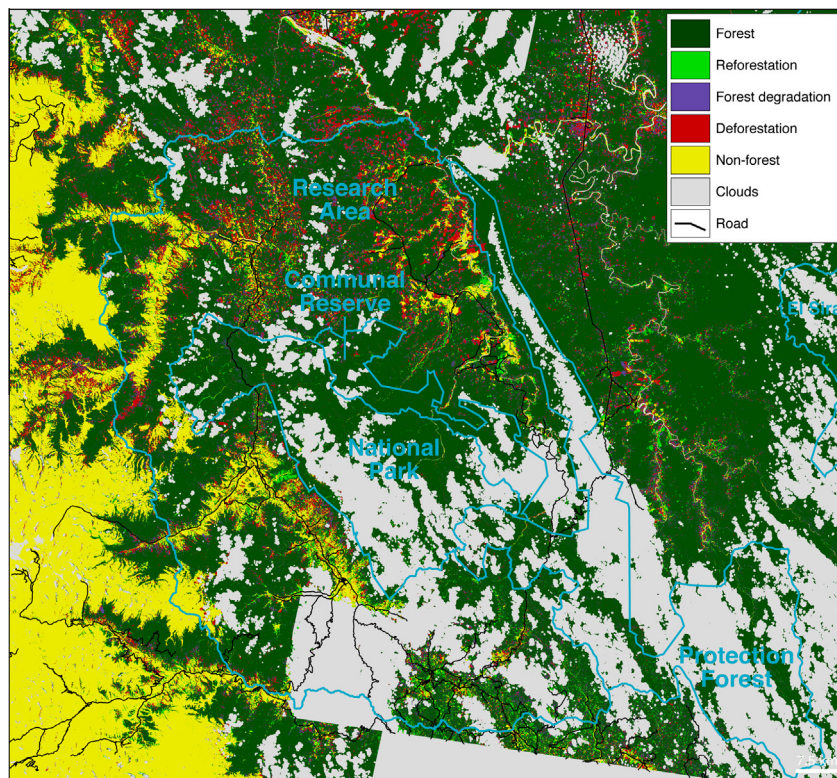


Fig. 4. Land cover change 1989–2005. Roads are shown as black lines. Research area and protected areas are shown with aqua lines.

The Selva Central secondary forest plots have recovered half the number of tree species of the old-growth forest plots and nearly half of the species are late-successional, suggesting a potential

for biodiversity conservation through natural regeneration. Forest restoration provides an important option to increase the extent of tropical forests and augment the provision of vital ecosystem

Table 5

Total aboveground live carbon in the Selva Central research area, carbon changes, and uncertainties calculated by Monte Carlo analysis. Historical results (1989–2005) come from field measurements and analysis of Landsat data. Carbon projections (2021) come from statistical relationships of historical deforestation and reforestation to environmental and social factors.

	Mean (10 ⁶ Mg C)	95% CI (10 ⁶ Mg C)	95% CI (%)
1989			
Old-growth forest	27.9	8.8	32
Secondary forest	1.6	0.5	31
Low vegetation	0.6	0.3	46
Sparse vegetation	0.2	0.07	38
Total	30.2	7.5	25
2005			
Old-growth forest	25.8	8.0	31
Secondary forest	1.9	0.7	36
Low vegetation	0.8	0.4	48
Sparse vegetation	0.2	0.05	33
Total	28.7	7.3	26
2021 (Projected)			
Old-growth forest	24.1	7.1	30
Secondary forest	2.2	0.6	29
Low vegetation	0.9	0.4	47
Sparse vegetation	0.2	0.07	38
Total	27.3	6.5	24
1989–2005			
Deforestation	–2.3	0.4	18
Reforestation	1.2	0.3	23
Forest degradation	–0.5	0.2	31
Non-forest accumulation	0.03	0.01	39
Net change	–1.6	0.4	26
2005–2021 (Projected)			
Deforestation	–2.2	0.6	28
Reforestation	1.4	0.4	31
Forest degradation	–0.6	0.2	33
Non-forest accumulation	~0	<0.01	35
Net change	–1.4	0.3	24

services to people (Lamb et al., 2005). In addition, the fraction of trees of old-growth species provides a potentially useful indicator to track the progress of forest restoration.

The significant positive correlation of aboveground live carbon density and species richness is consistent with findings from natural tropical forest on Barro Colorado Island, Panama (Ruiz-Jaen and Potvin, 2011). Our small sample compelled us to combine old-growth and secondary forest plots in the same analysis, so the correlation may in part reflect a relationship of carbon density with tree size, due to state of succession, rather than species richness. Still, a positive relationship of carbon density and species richness persists within the secondary forest plots. The correlation demonstrates how forest conservation produces two benefits: increased biodiversity and increased carbon storage. It also supports a previous finding that future tree species composition will strongly influence future carbon storage in tropical forests (Bunker et al., 2005). The information on biodiversity and carbon came from the same plots, demonstrating that plots can serve both purposes, consistent with recent findings (Baraloto et al., 2013).

4.2. Historical land cover changes

The 1989–2005 Selva Central deforestation rate of 0.3% y^{–1} was higher than the 2000–2005 Peruvian Amazon non-protected area deforestation rate of 0.2% y^{–1} (Oliveira et al., 2007). The Selva Central forest degradation rate of 0.2% y^{–1} that we found was the same as the rate that Oliveira et al. (2007) found for Peruvian Amazon non-protected areas. We evaluated degradation using an analytical method at the pixel level that was less intense computationally than the sub-pixel method (Asner et al., 2005) used by Oliveira

et al. (2007). The Selva Central deforestation rate matched the 2000–2005 deforestation rate from a remote sensing survey of South America (Asner et al., 2009). The rate was lower than the 2000–2005 deforestation rate of 0.7% y^{–1} across Brazil and 1.2% y^{–1} in Mato Grosso, Brazil (Hansen et al., 2010). In the Brazilian Amazon, expansion of export agriculture drives the high deforestation rate (Macedo et al., 2012), while in the Peruvian Amazon, structural adjustment of the economy, which has reduced agricultural subsidies, has reduced the rate of deforestation (Alvarez and Naughton-Treves, 2003). Landsat change detection identified local areas of forest change at a spatial resolution useful to natural resource managers (Fig. 6).

Distance to roads and distance to towns were, respectively, the first and second highest factors in explaining historical deforestation. The concentration of deforestation along roads and near towns (Fig. 4) confirms the finding. The probability of deforestation can double or triple close to roads and towns (Fig. A1). These results are consistent with multivariate analyses in the Brazilian legal Amazon that indicated a high correlation of deforestation to distance to highways and rural population density (Laurance et al., 2002), to remote sensing analyses across the tropics that indicated a high correlation of deforestation to urban population growth (DeFries et al., 2010), and to analyses in the Peruvian Amazon that identified proximity to towns as the most important factor explaining deforestation (Alvarez and Naughton-Treves, 2003). Research in Yungas cloud forests north of Selva Central has also found that tree species diversity declines close to tracks and roads (Ledo et al., 2009). Although distance to rivers was not as important, our analyses of Landsat data detected extensive deforestation along rivers, which occurs, for example, in the Palcazú River valley due to ease of transportation for agricultural operations (McClain and Cossío, 2003).

The extremely low rates of deforestation and forest degradation in the parts of the three protected areas within 5 km of roads and the higher rates outside the protected areas reveal that the protected areas have prevented deforestation and forest degradation. The protection forest was the only protected area with non-negligible forest degradation. There, the degradation rate was half the rate of the entire Selva Central research area, possibly due to illegal logging.

Our results support previous research that has shown the effectiveness of protected areas in preventing deforestation, including analyses of 150,000 km² of protected areas in the Peruvian Amazon (Oliveira et al., 2007), a subset of ten protected areas in the Peruvian Amazon (Vuohelainen et al., 2012), and majorities of 206 protected areas in the Brazilian Amazon (Soares-Filho et al., 2010), 150 protected areas in Costa Rica (Andam et al., 2008), 97 protected areas in Mexico (Figueroa and Sánchez-Cordero, 2008; Rayn and Sutherland, 2011), and 93 protected areas in 22 countries across the tropics (Bruner et al., 2001). At least four efforts (Andam et al., 2008; Bruner et al., 2001; Oliveira et al., 2007; Soares-Filho et al., 2010) explicitly analyzed the remoteness of protected areas and demonstrated that it is not the reason for lower deforestation. Higher deforestation rates in the areas outside of 70% of 292 protected areas showed increasing isolation of protected areas (DeFries et al., 2005).

On the other hand, a meta-analysis of articles on 40 protected areas and 33 community-managed forests found lower deforestation in the latter (Porter-Bolland et al., 2012). Those results may reflect a phenomenon observed in the Peruvian Amazon in which weak local governance can decrease the effectiveness of protection, whereas good relations with surrounding communities can increase effectiveness (Vuohelainen et al., 2012). Analysis of 292 protected areas in the Brazilian Amazon indicated that strict protection more effectively avoided deforestation than sustainable use (Nolte et al., 2013).

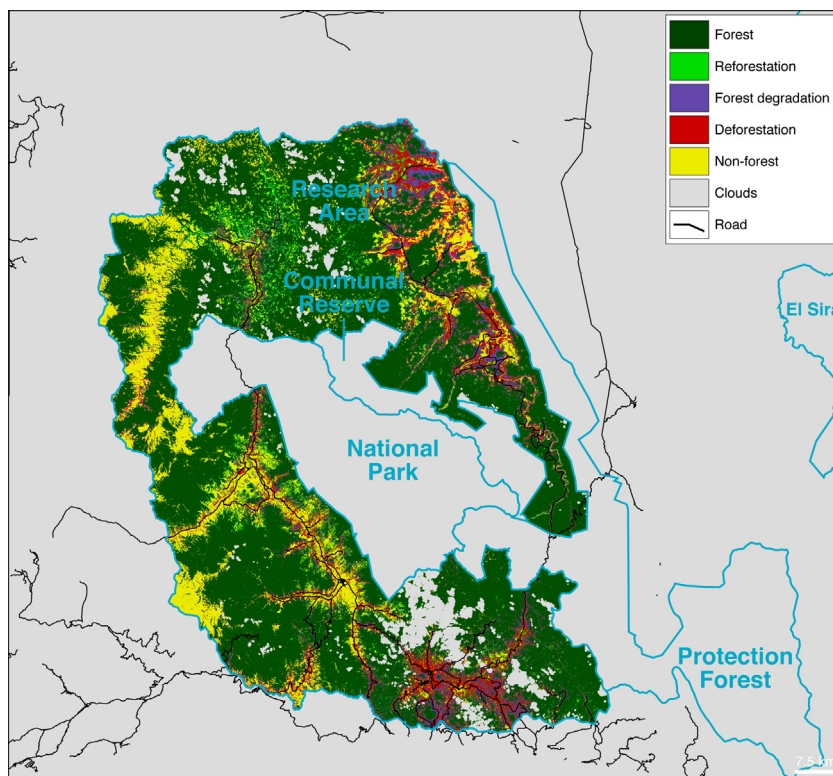


Fig. 5. Projected land cover change 2005–2021.

4.3. Forest carbon densities

Tree density and basal area, two ecosystem properties that determine forest carbon density, are one-third greater in the Selva Central old-growth plots than the average of a network of 50 Amazonian forest plots (Lewis et al., 2004) and two-thirds greater than a set of plots in the Brazilian Amazon (Rice et al., 2004). Tree density in the old-growth plots is 200 trees ha^{-1} higher than one estimate for the area in a model of the entire Amazon (ter Steege et al., 2003). The Selva Central secondary forest plots have lower tree density than a set of plots in Costa Rica, but the same basal area (Chazdon et al., 2005).

Selva Central old-growth and secondary forest carbon densities of $93 \pm 39 \text{ Mg ha}^{-1}$ and $40 \pm 10 \text{ Mg ha}^{-1}$, respectively, are nearly the same as the 90 Mg ha^{-1} and 33 Mg ha^{-1} estimated from Lidar remote sensing farther south in the Peruvian Amazon (ASner et al., 2010). The elevation gradient from lowland Amazon forest to montane Yungas forest in Selva Central does not show a clear trend in forest carbon density, in contrast to a gradient of decreasing carbon density with increasing elevation farther south in the Peruvian Amazon (Girardin et al., 2010). Selva Central old-growth forest carbon density is lower than the 120 Mg ha^{-1} estimated in a set of old-growth plots across the Amazon, but it is high compared to the carbon density estimated for the area in a model of the entire Amazon (Saatchi et al., 2007). Selva Central old-growth forest carbon density is lower than the average of $150 \pm 5 \text{ Mg ha}^{-1}$ found in a set of permanent monitoring plots across the Amazon (Baker et al., 2004b) and a set of permanent plots in Brazil (Chambers et al., 2001; Rice et al., 2004). Selva Central secondary forest carbon density is higher than the 25 Mg ha^{-1} estimated in a set of secondary forest plots across the Amazon (Saatchi et al., 2007).

Although 1989–2005 deforestation caused gross emissions of 2.3 ± 0.4 million Mg carbon, reforestation recaptured half that amount. This demonstrates the strength of natural regeneration

of forests in the Selva Central. Forest degradation, including degradation due to fires (Aragão and Shimabukuro, 2010), caused substantial emissions, but they were one-fifth of the magnitude of deforestation emissions.

4.4. Projected land cover and carbon changes

The probability analyses projected higher gross rates of deforestation and reforestation, leading to a slight projected decline in the net rate of deforestation for the research area. Future deforestation might cluster near roads, towns, and previously deforested areas, while projected reforestation might occur at more distant locations in areas recovering from agricultural clearing.

The multivariate projection method that we used is similar to methods tested in the Brazilian Amazon (Laurance et al., 2002; Soares-Filho et al., 2006; Yanai et al., 2012). We aimed to improve upon past efforts by using historical patterns of the influences of different factors on forest change, rather than making assumptions about future land use practices (de Barros Ferraz et al., 2005), and by projecting both the rate and location of potential future forest changes, in contrast to methods that assume a future deforestation rate (Pontius et al., 2001). Furthermore, we developed a method to estimate potential carbon benefits of avoided deforestation and reforestation projects, which previously have been treated separately.

Because the projections of future land cover do not use projections of future population growth, they may underestimate future deforestation. The factors determining future population density are, however, so complex that reliable spatial projections of future patterns of population do not yet exist. The land cover projections reflect potential trends based on initial conditions. We did not attempt to project leakage (unintended shifting of emissions to locations outside the analysis area), but instead provide projections of potential emissions or removals.

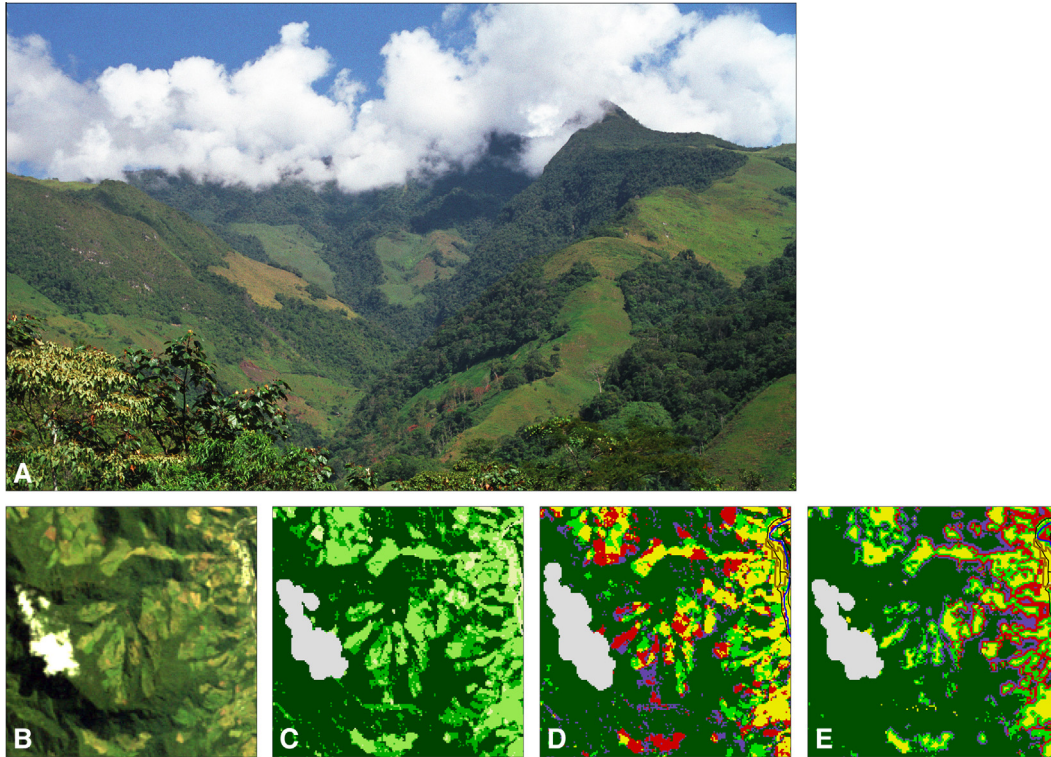


Fig. 6. View of a 5 km × 5 km square area of the Selva Central centered on 10.08° S, 75.57° W, west of the town of Pozuzo. (a) Photograph from the ground, looking from near the northeast corner towards the southwest. (b) Landsat real-color image. (c) Aboveground carbon and land cover 2005 (see Fig. 3 legend). (d) Land cover change 1989–2005 (see Fig. 4 legend; brown = Pozuzo, blue = river). (e) Projected land cover change 2005–2021.

For a CDM afforestation or reforestation activity, the land area available is the area of non-forest cover since 1990: 13% of the area. If an organization developed a CDM project activity in the research area, they could receive credit for carbon storage occurring above the projected 2005–2021 baseline gross reforestation rate: $1.8\% \text{ y}^{-1}$. For a CDM activity, local communities in the Selva Central and external partners have considered one practice that would combine reforestation with agriculture: contour hedgerow intercropping (*fajas de enriquecimiento*; Alegre and Rao, 1996). The carbon benefits would depend on the surface area and survival rate of the plantations.

The maximum projected potential benefit of a REDD+ project is the projected amount of emissions from gross deforestation and gross degradation: 2.8 ± 0.8 million Mg carbon. A REDD+ project in the Selva Central would require close local cooperation (Scriven, 2012) and extension of forestry practices that do not involve clear-cutting. A REDD+ forest conservation project in the Selva Central could avoid greenhouse gas emissions equivalent to the 2011 emissions of 480,000 residents of the United States (US EPA, 2013).

4.5. Uncertainties of forest carbon estimates

Our Monte Carlo analyses answered the key question of whether or not the estimated carbon emissions were statistically significant. Because our results show that the entire range of values of 1989–2005 net carbon change was negative (–1.2 to –2.0 million Mg), we conclude that the net emissions were significant. While the 95% CIs of the carbon stock estimates for individual years show some overlap, the proper measure for evaluating the significance of carbon change is the directly-calculated 95% CI of the 1989–2005 net carbon change, which showed that the entire range of values was less than zero. While the significance of net carbon emissions is not necessarily surprising, quantification of

the uncertainty provides strong evidence of one impact of extensive deforestation in the Selva Central.

The uncertainties of forest carbon density estimates for Selva Central of 24–42% were higher than the uncertainties of ~5% reported for other field inventory plots across the Amazon (Baker et al., 2004b) and in Brazil (Chambers et al., 2001; Rice et al., 2004), but those other estimates did not analyze allometric and carbon fraction uncertainties, nor did they use Monte Carlo analysis. If other efforts were to re-calculate forest carbon densities and stocks to include the major sources of uncertainty that we have evaluated, the uncertainties of their estimates would increase, implying current overestimation of emissions or sequestration. The 0.50 carbon fraction of biomass that many others commonly use, with no error estimate, already introduces up to 6% uncertainty when compared to the 0.47 carbon fraction of biomass derived from a meta-analysis of published estimates from around the world (McGroddy et al., 2004) and used in the IPCC National Greenhouse Gas Inventory Guidelines (Aalde et al., 2006).

The Monte Carlo analyses offer a quantitative threshold for policymakers who will need to decide on the amount of carbon savings to estimate at the beginning of a REDD+ project for the actual carbon successfully stored by the end of a 20–30 year project. The Selva Central projected 2005–2021 gross emissions from deforestation and degradation are 2.0–3.6 million Mg. A REDD+ project could decide to claim the central estimate (2.8 million Mg), with the justification that the estimate directly emerges from the mean values of all the variables, or the project could claim the low estimate, a safer approach that would hedge against unforeseeable future events that might reduce estimated carbon storage.

Our sensitivity analyses of the Monte Carlo estimates of uncertainty respond to the key question of what improvements

in methods or specific variables could most reduce overall uncertainty in the future. Because the allometric equations accounted for most of the overall uncertainty of forest carbon density estimates, the development of more precise species- or taxon-specific allometric equations could most reduce uncertainty. Diameter measurement error in our field inventories accounted for the lowest fraction of uncertainty, so it is important to attain the accuracy of field measurements that we achieved. The uncertainty of the carbon density in old-growth plots was double the uncertainty in secondary forest, which had double the number of plots. Either the secondary forest plots were more similar than the old-growth plots or the larger sample size reduced the uncertainty. In any case, more field plots would provide a more representative sample.

Because remote sensing inaccuracy accounted overwhelmingly for uncertainty of carbon change estimates, improved accuracy of land cover classification would most reduce overall uncertainty. Indeed, the fraction of uncertainty due to remote sensing was so high that improvements to field measurements, wood densities, carbon fractions, and allometric equations would have had virtually no effect on our carbon change uncertainty estimates.

Although the Monte Carlo analyses took time and effort, they provided useful information on the significance of forest carbon changes and on improvements to reduce overall uncertainty.

5. Conclusion

Using field measurements, Landsat remote sensing, and Monte Carlo analyses, we have shown that:

1. Selva Central old-growth forest has higher tree species richness than many tropical forests and all temperate forests.
2. Deforestation reduced old-growth forest cover from three-quarters of the Selva Central research area in 1989 to two-thirds in 2005.
3. Deforestation and forest degradation caused net emissions of 1.6 ± 0.4 million Mg carbon, a loss that the Monte Carlo analyses of uncertainty showed was statistically significant.
4. The three protected areas (Parque Nacional Yanachaga-Chemillén, Reserva Comunal Yanasha, Bosque de Protección San Matías-San Carlos) have prevented deforestation and forest degradation.
5. Effective forest conservation could avoid emissions of 2.8 ± 0.8 million Mg carbon under a REDD+ project, equivalent to the annual emissions of 480,000 residents of the US.

Acknowledgements

We thank Jaime Fernandez-Baca and Bill Stanley. We thank the field inventory crew – Edson Albegrín K., Emilio Astupiñán O., Tullio Chávez E., Elvis Giraldo F., Angel Köhle G., Máximiliano Luján, Jesús Mosquera E., Gilmer Pretell V., Bernavé Ramos R., Elías Schmidt A., Alejandro Sebastián L., Eligio Toribio, Edico Valerio, Jimmy Vogt C. – and other inventory staff – Joyer Bastidas, Jimmy Bottger Y., Carlos Estrella H., Julio de la Torre V., Marianela Velita B., Biviana Yantas.

We gratefully acknowledge data shared by Paulo J.C. Oliveira and Gregory P. Asner, support from Christine A. Rose, and funding from the National Energy Technology Laboratory of the U.S. Department of Energy (Cooperative Agreement DE-FC-26-01NT41151), the Nature Conservancy, ProNaturaleza, and the College of Natural Resources of the University of California, Berkeley.

Appendix A. Supplementary material

Supplementary material associated with this article can be found, in the online version, at <http://dx.doi.org/10.1016/j.for-eco.2013.10.019>.

References

- Aalde, H., Gonzalez, P., Gytarsky, M., Krug, T., Kurz, W.A., Ogle, S., Raison, J., Schoene, D., Ravindranath, N.H., Elhassan, N.G., Heath, L.S., Higuchi, N., Kainja, S., Matsumoto, M., Sánchez, M.J.S., Somogyi, Z., 2006. Forest land. In: Intergovernmental Panel on Climate Change, National Greenhouse Gas Inventory Guidelines. Institute for Global Environmental Strategies, Hayama, Japan.
- Alegre, J.C., Rao, M.R., 1996. Soil and water conservation by contour hedging in the humid tropics of Peru. *Agriculture, Ecosystems, and Environment* 57, 17–25.
- Alvarez, N.L., Naughton-Treves, L., 2003. Linking national agrarian policy to deforestation in the Peruvian Amazon: A case study of Tambopata, 1986–1997. *Ambio* 32, 269–274.
- Andam, K.S., Ferraro, P.J., Pfaff, A., Sanchez-Azofeifa, G.A., Robalino, J.A., 2008. Measuring the effectiveness of protected area networks in reducing deforestation. In: *Proceedings of the National Academy of Sciences of the USA* 105. pp. 16089–16094.
- Aragão, L.E.O.C., Shimabukuro, Y.E., 2010. The incidence of fire in Amazonian forests with implications for REDD. *Science* 328, 1275–1278.
- Aróstegui, A., 1974. Características tecnológicas y usos de la madera de 145 especies del país. Universidad Nacional Agraria La Molina (UNALM), Lima, Peru.
- Asner, G.P., Knapp, D.E., Broadbent, E.N., Oliveira, P.J.C., Keller, M., Silva, J.N., 2005. Selective logging in the Brazilian Amazon. *Science* 310, 480–482.
- Asner, G.P., Rudel, T.K., Aide, M., DeFries, R., Emerson, R., 2009. A contemporary assessment of change in humid tropical forests. *Conservation Biology* 23, 1386–1395.
- Asner, G.P., Powell, G.V.N., Mascaró, J., Knapp, D.E., Clark, J.K., Jacobson, J., Kennedy-Bowdoin, T., Balaji, A., Paez-Acosta, G., Victoria, E., Secada, L., Valqui, M., Hughes, R.F., 2010. High-resolution forest carbon stocks and emissions in the Amazon. In: *Proceedings of the National Academy of Sciences of the USA* 107. pp. 16738–16742.
- Baccini, A., Goetz, S.J., Walker, W.S., Laporte, N.T., Sun, M., Sulla-Menashe, D., Hackler, J., Beck, P.S.A., Dubayah, R., Friedl, M.A., Samanta, S., Houghton, R.A., 2012. Estimated carbon dioxide emissions from tropical deforestation improved by carbon-density maps. *Nature Climate Change* 2, 182–185.
- Baker, T.R., Phillips, O.L., Malhi, Y., Almeida, S., Arroyo, L., Di Fiore, A., Erwin, T., Killeen, T.J., Laurance, S.G., Laurance, W.F., Lewis, S.L., Lloyd, J., Monteagudo, A., Neill, D.A., Patiño, S., Pitman, N.C.A., Silva, J.N.M., Martínez, R.V., 2004a. Variation in wood density determines spatial patterns in Amazonian forest biomass. *Global Change Biology* 10, 545–562.
- Baker, T.R., Phillips, O.L., Malhi, Y., Almeida, S., Arroyo, L., Di Fiore, A., Erwin, T., Higuchi, N., Killeen, T.J., Laurance, S.G., Laurance, W.F., Lewis, S.L., Monteagudo, A., Neill, D.A., Vargas, P.N., Pitman, N.C.A., Silva, J.N.M., Martínez, R.V., 2004b. Increasing biomass in Amazonian forest plots. *Philosophical Transactions of the Royal Society of London B* 359, 353–365.
- Baraloto, C., Molto, Q., Rabaud, S., Hérault, B., Valencia, R., Blanc, L., Fine, P.V.A., Thompson, J., 2013. Rapid simultaneous estimation of aboveground biomass and tree diversity across Neotropical forests: A comparison of field inventory methods. *Biotropica* 45, 288–298.
- Bicheron, P., Defourny, P., Brockmann, C., Schouten, L., Vancutsem, C., Huc, M., Bontemps, S., Leroy, M., Achard, F., Herold, M., Ranera, F., Arino, O., 2008. Globcover: Products Description and Validation Report. Médias-France, Toulouse, France.
- Brako, L., Zarucchi, J.L., 1993. Catalogue of the Flowering Plants and Gymnosperms of Peru (Catálogo de las angiospermas y gimnospermas del Perú). Missouri Botanical Garden, St. Louis, Missouri.
- Bruner, A.G., Gullison, R.E., Rice, R.E., da Fonseca, G.A.B., 2001. Effectiveness of parks in protecting tropical biodiversity. *Science* 291, 125–128.
- Bunker, D.E., DeClerck, F., Bradford, J.C., Colwell, R.K., Perfecto, I., Phillips, O.L., Sankaran, M., Naeem, S., 2005. Species loss and aboveground carbon storage in a tropical forest. *Science* 310, 1029–1031.
- Cardinale, B.J., Duffy, J.E., Gonzalez, A., Hooper, D.U., Perrings, C., Venail, P., Narwani, A., Mace, G.M., Tilman, D., Wardle, D.A., Kinzig, A.P., Daily, G.C., Loreau, M., Grace, J.B., Larigauderie, A., Srivastava, D.S., Naeem, S., 2012. Biodiversity loss and its impact on humanity. *Nature* 486, 59–67.
- Chambers, J.Q., dos Santos, J., Ribeiro, R.J., Higuchi, N., 2001. Tree damage, allometric relationships, and above-ground net primary production in a tropical forest. *Forest Ecology and Management* 152, 73–84.
- Chave, J., Condit, R., Aguilar, S., Hernandez, A., Lao, S., Perez, R., 2004. Error propagation and scaling for tropical forest biomass estimates. *Philosophical Transactions of the Royal Society of London B* 359, 409–420.
- Chave, J., Muller-Landau, H.C., Baker, T.R., Easdale, T.A., ter Steege, H., Webb, C.O., 2006. Regional and phylogenetic variation of wood density across 2456 neotropical tree species. *Ecological Applications* 16, 2356–2367.
- Chazdon, R.L., Brenes, A.R., Alvarado, B.V., 2005. Effects of climate and stand age on annual tree dynamics in tropical second-growth rain forests. *Ecology* 86, 1808–1815.

- Condit, R., Pitman, N., Leigh, E.G., Chave, J., Terborgh, J., Foster, R.B., Núñez, P., Aguilar, S., Valencia, R., Villa, G., Muller-Landau, H.C., Losos, E., Hubbell, S.P., 2002. Beta-diversity in tropical forest trees. *Science* 295, 666–669.
- de Barros Ferraz, S.F., Vettorazzi, C.A., Theobald, D.M., Ballester, M.V.R., 2005. Landscape dynamics of Amazonian deforestation between 1984 and 2002 in central Rondônia, Brazil: assessment and future scenarios. *Forest Ecology and Management* 204, 69–85.
- DeFries, R., Hansen, A., Newton, A.C., Hansen, M.C., 2005. Increasing isolation of protected areas in tropical forests over the past twenty years. *Ecological Applications* 15, 19–26.
- DeFries, R.S., Rudel, T., Uriarte, M., Hansen, M., 2010. Deforestation driven by urban population growth and agricultural trade in the twenty-first century. *Nature Geoscience* 3, 178–181.
- Food and Agriculture Organization (FAO), 2011. *State of the World's Forests 2011*. FAO, Rome, Italy.
- Fearnside, P.M., 1997. Wood density for estimating forest biomass in Brazilian Amazonia. *Forest Ecology and Management* 90, 59–87.
- Figuerola, F., Sánchez-Cordero, V., 2008. Effectiveness of natural protected areas to prevent land use and land cover change in Mexico. *Biodiversity and Conservation* 17, 3223–3240.
- Gentry, A., 1988. Changes in plant community diversity and floristic composition on environmental and geographical gradients. *Annals of the Missouri Botanical Garden* 75, 1–34.
- Gentry, A., 1993. Overview of the Peruvian flora. In: Brako, L., Zarucchi, J.L. (Eds.), *Catalogue of the Flowering Plants and Gymnosperms of Peru (Catálogo de las angiospermas y gimnospermas del Perú)*. Missouri Botanical Garden, St. Louis, Missouri.
- Gibbon, A., Silman, M.R., Malhi, Y., Fisher, J.B., Meir, P., Zimmermann, M., Dargie, G.C., Farfan, W.R., Garcia, K.C., 2010. Ecosystem carbon storage across the grassland-forest transition in the high Andes of Manu National Park, Peru. *Ecosystems* 13, 1097–1111.
- Gibbs, H.K., Ruesch, A.S., Achard, F., Clayton, M.K., Holmgren, P., Ramankutty, N., Foley, J.A., 2010. Tropical forests were the primary sources of new agricultural land in the 1980s and 1990s. In: *Proceedings of the National Academy of Sciences of the USA* 107, pp. 16732–16737.
- Gibson, L., Lee, T.M., Koh, L.P., Brook, B.W., Gardner, T.A., Barlow, J., Peres, C.A., Bradshaw, C.J.A., Laurance, W.F., Lovejoy, T.E., Sodhi, N.S., 2011. Primary forests are irreplaceable for sustaining tropical biodiversity. *Nature* 478, 378–381.
- Girardin, C.A.J., Malhi, Y., Aragão, L.E.O.C., Mamani, M., Huaraca Huasco, W., Durand, L., Feeley, K.J., Rapp, J., Silva-Espejo, J.E., Silman, M., Salinas, N., Whittaker, R.J., 2010. Net primary productivity allocation and cycling of carbon along a tropical forest elevational transect in the Peruvian Andes. *Global Change Biology* 16, 3176–3192.
- Gonzalez, P., Asner, G.P., Battles, J.J., Lefsky, M.A., Waring, K.M., Palace, M., 2010a. Forest carbon densities and uncertainties from Lidar, QuickBird, and field measurements in California. *Remote Sensing of Environment* 114, 1561–1575.
- Gonzalez, P., Neilson, R.P., Lenihan, J.M., Drapek, R.J., 2010b. Global patterns in the vulnerability of ecosystems to vegetation shifts due to climate change. *Global Ecology and Biogeography* 19, 755–768.
- Gutman, G., Huang, C., Chandler, G., Noojipady, P., Masek, J.G., 2013. Assessment of the NASA-USGS Global Land Survey (GLS) datasets. *Remote Sensing of Environment* 134, 249–265.
- Hamlin, C.C., Salick, J., 2003. Yanasha agriculture in the upper Peruvian Amazon: persistence and change fifteen years down the 'road'. *Economic Botany* 57, 163–180.
- Hansen, M.C., Stehman, S.V., Potapov, P.V., 2010. Quantification of global gross forest cover loss. In: *Proceedings of the National Academy of Sciences of the USA* 107, pp. 8650–8655.
- Harris, N.L., Brown, S., Hagen, S.C., Saatchi, S.S., Petrova, S., Salas, W., Hansen, M.C., Potapov, P.V., Lutsch, A., 2012. Baseline map of carbon emissions from deforestation in tropical regions. *Science* 336, 1573–1576.
- Intergovernmental Panel on Climate Change (IPCC), 2006. *Agriculture, forestry, and other land use*. In: IPCC, *National Greenhouse Gas Inventory Guidelines*. Institute for Global Environmental Strategies, Hayama, Japan.
- Joppa, L.N., Roberts, D.L., Myers, N., Pimm, S.L., 2011. Biodiversity hotspots house most undiscovered plant species. In: *Proceedings of the National Academy of Sciences of the USA* 108, pp. 13171–13176.
- Lamb, D., Erskine, P.D., Parrotta, J.A., 2005. Restoration of degraded tropical forest landscapes. *Science* 310, 1628–1632.
- Latham, R.E., Ricklefs, R.E., 1993. Global patterns of tree species richness in moist forests: energy-diversity theory does not account for variation in species richness. *Oikos* 67, 325–333.
- Laurance, W.F., Albernaz, A.K.M., Schroth, G., Fearnside, P.M., Bergen, S., Venticinque, E.M., Da Costa, C., 2002. Predictors of deforestation in the Brazilian Amazon. *Journal of Biogeography* 29, 1–12.
- Laurance, W.F., Oliveira, A.A., Laurance, S.G., Condit, R., Nascimento, H.E.M., Sanchez-Thorin, A.C., Lovejoy, T.E., Andrade, A., D'Angelo, S., Ribeiro, J.E., Dick, C.W., 2004. Pervasive alteration of tree communities in undisturbed Amazonian forests. *Nature* 428, 171–175.
- Laurance, W.F., Nascimento, H.E.M., Laurance, S.G., Andrade, A., Ribeiro, J.E.L.S., Giraldo, J.P., Lovejoy, T.E., Condit, R., Chave, J., Harms, K.E., D'Angelo, S., 2006. Rapid decay of tree-community composition in Amazonian forest fragments. In: *Proceedings of the National Academy of Sciences of the USA* 103, pp. 19010–19014.
- Le Quéré, C., Andres, R.J., Boden, T., Conway, T., Houghton, R.A., House, J.I., Marland, G., Peters, G.P., van der Werf, G.R., Ahlström, A., Andrew, R.M., Bopp, L., Canadell, J.G., Ciais, P., Doney, S.C., Enright, C., Friedlingstein, P., Huntingford, C., Jain, A.K., Jourdain, C., Kato, E., Keeling, R.F., Klein Goldewijk, K., Levis, S., Levy, P., Lomas, M., Poulter, B., Raupach, M.R., Schwinger, J., Sitch, S., Stocker, B.D., Viovy, N., Zaehle, S., Zeng, N., 2013. The global carbon budget 1959–2011. *Earth System Science Data* 5, 165–185.
- Ledo, A., Montes, F., Condes, S., 2009. Species dynamics in a montane cloud forest: identifying factors involved in changes in tree diversity and functional characteristics. *Forest Ecology and Management* 258, S75–S84.
- Lewis, S.L., Phillips, O.L., Baker, T.R., Lloyd, J., Malhi, Y., Almeida, S., Higuchi, N., Laurance, W.F., Neill, D.A., Silva, J.N.M., Terborgh, J., Lezama, A.T., Martinez, R.V., Brown, S., Chave, J., Kuebler, C., Vargas, P.N., Vinceti, B., 2004. Concerted changes in tropical forest structure and dynamics: evidence from 50 South American long-term plots. *Philosophical Transactions of the Royal Society of London B* 359, 421–436.
- Macedo, M.N., DeFries, R.S., Morton, D.C., Stickler, C.M., Galford, G.L., Shimabukuro, Y.E., 2012. Decoupling of deforestation and soy production in the southern Amazon during the late 2000s. In: *Proceedings of the National Academy of Sciences of the USA* 109, pp. 1341–1346.
- McClain, M.E., Cossío, R.E., 2003. The use and conservation of riparian zones in the rural Peruvian Amazon. *Environmental Conservation* 30, 242–248.
- McGroddy, M.E., Daufresne, T., Hedin, L.O., 2004. Scaling of C:N:P stoichiometry in forests worldwide: implications of terrestrial Redfield-type ratios. *Ecology* 85, 2390–2401.
- Mitchell, T.D., Jones, P.D., 2005. An improved method of constructing a database of monthly climate observations and associated high-resolution grids. *International Journal of Climatology* 25, 693–712.
- Monni, S., Peltoniemi, M., Palosuo, T., Lehtonen, A., Mäkipää, R., Savolainen, I., 2007. Uncertainty of forest carbon stock changes – implications to the total uncertainty of GHG inventory of Finland. *Climatic Change* 81, 391–413.
- Nelson, R., Holben, B., 1986. Identifying deforestation in Brazil using multiresolution satellite data. *International Journal of Remote Sensing* 7, 429–448.
- Nelson, B.W., Mesquita, R., Pereira, J.L.G., de Souza, S.G.A., Batista, G.T., Couto, L.B., 1999. Allometric regressions for improved estimate of secondary forest biomass in the central Amazon. *Forest Ecology and Management* 117, 149–167.
- Nolte, C., Agrawal, A., Silvius, K.M., Soares-Filho, B.S., 2013. Governance regime and location influence avoided deforestation success of protected areas in the Brazilian Amazon. In: *Proceedings of the National Academy of Sciences of the USA* 110, pp. 4956–4961.
- Oliveira, P.J.C., Asner, G.P., Knapp, D.E., Almeyda, A., Galván-Gildemeister, R., Keene, S., Raybin, R.F., Smith, R.C., 2007. Land-use allocation protects the Peruvian Amazon. *Science* 317, 1233–1236.
- Palm, C., Tomich, T., Van Noordwijk, M., Vosti, S., Gockowski, J., Alegre, J., Verchot, L., 2004. Mitigating GHG emissions in the humid tropics: case studies from the Alternatives to Slash-and-Burn program (ASB). *Environment, Development, and Sustainability* 6, 145–162.
- Pan, Y., Birdsey, R.A., Fang, J., Houghton, R., Kauppi, P.E., Kurz, W.A., Phillips, O.L., Shvidenko, A., Lewis, S.L., Canadell, J.G., Ciais, P., Jackson, R.B., Pacala, S.W., McGuire, A.D., Piao, S., Rautiainen, A., Sitch, S., Hayes, D., 2011. A large and persistent carbon sink in the world's forests. *Science* 333, 988–993.
- Peña-Claros, M., 2003. Changes in forest structure and species composition during secondary forest succession in the Bolivian Amazon. *Biotropica* 35, 450–461.
- Phillips, O.L., Hall, P., Gentry, A.H., Sawyer, S.A., Vásquez, R., 1994. Dynamics and species richness of tropical rain forests. In: *Proceedings of the National Academy of Sciences of the USA* 91, pp. 2805–2809.
- Pitman, N.C.A., Terborgh, J.W., Silman, M.R., Vargas, P.N., Neill, D.A., Cerón, C.E., Palacios, W.A., Aulestia, M., 2002. A comparison of tree species diversity in two upper Amazonian forests. *Ecology* 83, 3210–3224.
- Pontius, R.G., Cornell, J.D., Hall, C.A.S., 2001. Modeling the spatial pattern of land-use change with GEOMOD2: application and validation for Costa Rica. *Agriculture, Ecosystems, and Environment* 85, 191–203.
- Porter-Bolland, L., Ellis, E.A., Guariguata, M.R., Ruiz-Mallén, I., Negrete-Yankelevich, S., Reyes-García, V., 2012. Community managed forests and forest protected areas: an assessment of their conservation effectiveness across the tropics. *Forest Ecology and Management* 268, 6–17.
- Rayn, D., Sutherland, W.J., 2011. Impact of nature reserve establishment on deforestation: a test. *Biodiversity and Conservation* 20, 1625–1633.
- Rice, A.H., Pyle, E.H., Saleska, S.R., Hutyrá, L., Palace, M., Keller, M., De Camargo, P.B., Portilho, K., Marques, D.F., Wofsy, S.C., 2004. Carbon balance and vegetation dynamics in an old-growth Amazonian forest. *Ecological Applications* 14, S55–S71.
- Richards, P.W., 1996. *The Tropical Rain Forest*, Second ed. Cambridge University Press, Cambridge, UK.
- Ruiz-Jaen, M.C., Potvin, C., 2011. Can we predict carbon stocks in tropical ecosystems from tree diversity? Comparing species and functional diversity in a plantation and a natural forest. *New Phytologist* 189, 978–987.
- Saatchi, S.S., Houghton, R.A., dos Santos Alvalá, R.C., Soares, J.V., Yu, Y., 2007. Distribution of aboveground live biomass in the Amazon basin. *Global Change Biology* 13, 816–837.
- Saatchi, S., Marlier, M., Chazdon, R.L., Clark, D.B., Russell, A.E., 2011. Impact of spatial variability of tropical forest structure on radar estimation of aboveground biomass. *Remote Sensing of Environment* 115, 2836–2849.

- Santos-Granero, F., Barclay, F., 1998. *Selva Central: History, Economy, and Land Use in Peruvian Amazonia*. Smithsonian Institution Press, Washington, DC.
- Scriven, J.N.H., 2012. Preparing for REDD: forest governance challenges in Peru's Central Selva. *Journal of Sustainable Forestry* 31, 421–444.
- Soares-Filho, B.S., Nepstad, D.C., Curran, L.M., Cerqueira, G.C., Garcia, R.A., Ramos, C.A., Voll, E., McDonald, A., Lefebvre, P., Schlesinger, P., 2006. Modelling conservation in the Amazon basin. *Nature* 440, 520–523.
- Soares-Filho, B., Moutinho, P., Nepstad, D., Anderson, A., Rodrigues, H., Garcia, R., Dietzsch, L., Merry, F., Bowman, M., Hissa, L., Silvestrini, R., Maretti, C., 2010. Role of Brazilian Amazon protected areas in climate change mitigation. In: *Proceedings of the National Academy of Sciences of the USA* 107, pp. 10821–10826.
- Sólymos, P., Lele, S.R., 2012. Global pattern and local variation in species–area relationships. *Global Ecology and Biogeography* 21, 109–120.
- ter Steege, H., Pitman, N., Sabatier, D., Castellanos, H., van der Hout, P., Daly, D.C., Silveira, M., Phillips, O., Vasquez, R., Van Andel, T., Duivenvoorden, J., De Oliveira, A.A., Ek, R., Lilwah, R., Thomas, R., Van Essen, J., Baider, C., Maas, P., Mori, S., Terborgh, J., Núñez Vargas, P., Mogollón, H., Morawetz, W., 2003. A spatial model of tree alpha-diversity and density for the Amazon region. *Biodiversity and Conservation* 12, 2255–2277.
- Terborgh, J., Andresen, E., 1998. The composition of Amazonian forests: patterns at local and regional scales. *Journal of Tropical Ecology* 14, 645–664.
- Terborgh, J., Foster, R.B., Núñez Vargas, P., 1996. Tropical tree communities: a test of the nonequilibrium hypothesis. *Ecology* 77, 561–567.
- Uhl, C., Buschbacher, R., Serrão, E.A.S., 1988. Abandoned pastures in eastern Amazonia. I. Patterns of plant succession. *Journal of Ecology* 76, 663–681.
- U.S. Environmental Protection Agency (US EPA), 2013. *Inventory of U.S. Greenhouse Gas Emissions and Sinks: 1990–2011*. US EPA Report 430-R-13-001, Washington, DC.
- van der Werff, H., Consiglio, T., 2004. Distribution and conservation significance of endemic species of flowering plants in Peru. *Biodiversity and Conservation* 13, 1699–1713.
- Vuohelainen, A.J., Coad, L., Marthews, T.R., Malhi, Y., Killeen, T.J., 2012. The effectiveness of contrasting protected areas in preventing deforestation in Madre de Dios, Peru. *Environmental Management* 50, 645–663.
- Whittaker, R.H., 1972. Evolution and the measurement of species diversity. *Taxon* 21, 213–251.
- Yanai, A.M., Fearnside, P.M., de Alencastro, Lima, Graça, P.M., Nogueira, E.M., 2012. Avoided deforestation in Brazilian Amazonia: simulating the effect of the juma sustainable development reserve. *Forest Ecology and Management* 282, 78–91.